Journal of Cleaner Production 541 (2026) 147531

Contents lists available at ScienceDirect

Journal of Cleaner Production

journal homepage: www.elsevier.com/locate/jclepro

# Local volcanic pozzolans from the Canary Islands as low-carbon cement substitutes: Linking microstructure, performance and $CO_2$ reduction

Juan J. Santana [a,*], Luis E. Hernández-Gutiérrez [b,c], Ignacio Nuez [d], Jiri Libich [e], Ricardo A. Liria-Romero [a], Ricardo M. Souto [f,g,**]

[a] Department of Process Engineering, Universidad de Las Palmas de Gran Canaria, E-35017, Las Palmas de Gran Canaria, Spain
[b] Regional Ministry of Public Works, Housing and Mobility, Government of the Canary Islands, E-38071, Santa Cruz de Tenerife, Spain
[c] Instituto Volcanológico de Canarias (INVOLCAN), E-38400, Puerto de la Cruz, Spain
[d] Department of Electronic Engineering and Automation, Universidad de Las Palmas de Gran Canaria, E-35017, Las Palmas de Gran Canaria, Spain
[e] Brno University of Technology, Faculty of Electrical Engineering and Communication, Department of Electrical and Electronic Technology, Technická 12, 61600, Brno, Czech Republic
[f] Department of Chemistry, Universidad de La Laguna, E-38200, La Laguna, Spain
[g] Institute of Materials and Nanoscience, Universidad de La Laguna, E-38200, La Laguna, Spain

## HIGHLIGHTS

- Quarry residues valorized locally, enabling circular economy in the Canaries.
- LCA estimates ~13.6 % GWP reduction per tonne of binder at 20 % replacement.
- Microstructure shows glassy matrices and reactive zeolitic phases.
- 20 % cement replacement meets ≥25 MPa compressive strength requirement.
- Results support low-carbon mortars compliant with UNE-EN performance specs.

## GRAPHICAL ABSTRACT

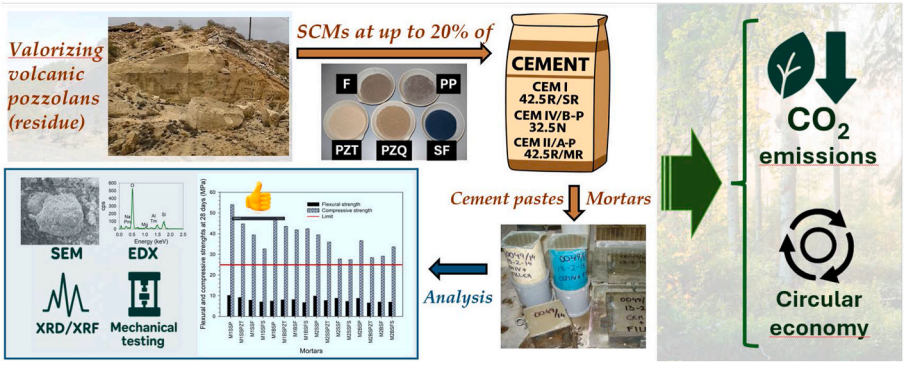


## ARTICLE INFO

*Keywords:*
Volcanic pozzolan
Clinker substitution
Low-carbon mortars
Circular economy
Life-cycle assessment
Cleaner production

## ABSTRACT

The cement industry contributes a significant share of global $CO_2$ emissions, positioning clinker substitution as a priority pathway for decarbonization. This study evaluates local volcanic pozzolans from the Canary Islands—both natural pyroclastic deposits and quarry residues—as supplementary cementitious materials. A comprehensive morphological and compositional characterization of the mortars was conducted using optical and scanning electron microscopies, energy-dispersive X-ray spectrometry, and X-ray diffraction and fluorescence analysis, as well as their mechanical testing. The pozzolans display trachytic–phonolitic–rhyolitic compositions with abundant zeolitic phases and amorphous content, meeting ASTM C618 Class N criteria. Mortars with up to 20 % cement replacement achieve compressive strengths above 25 MPa in line with UNE-EN 998-2, while flexural strength remains satisfactory. A cradle-to-gate assessment indicates that a 20 % clinker

* Corresponding author. Department of Process Engineering, Universidad de Las Palmas de Gran Canaria, E-35017, Las Palmas de Gran Canaria, Spain.
** Corresponding author. Department of Chemistry, Universidad de La Laguna, E-38200, La Laguna, Spain.
*E-mail addresses:* juan.santana@ulpgc.es (J.J. Santana), rsouto@ull.es (R.M. Souto).

https://doi.org/10.1016/j.jclepro.2026.147531
Received 14 October 2025; Received in revised form 11 December 2025; Accepted 9 January 2026
Available online 14 January 2026

substitution can lower the Global Warming Potential by approximately 13.6 % per tonne of binder. The results demonstrate that valorizing local volcanic resources enables meaningful $CO_2$ reductions without compromising structural applicability, thus supporting cleaner production in island and volcanic contexts.

## 1. Introduction

Reducing the carbon footprint of cement and concrete is essential to achieve near-term climate targets. Among the portfolio of mitigation measures, partial clinker substitution with supplementary cementitious materials (SCM) offers a readily deployable route that can deliver immediate $CO_2$ abatement while maintaining performance for structural and masonry applications. Natural pozzolans of volcanic origin are an attractive option in volcanic and insular territories due to proximity, availability, and their intrinsic reactivity (González-Morales et al., 2025).

Volcanic pozzolans have been widely studied as supplementary cementitious materials for the formulation of mortars and concretes because of their pozzolanic activity (Ababneh and Matalkah, 2018; Abiodun et al., 2022; Costafreda et al., 2021; Fazilati and Mohammadi Golafshani, 2020; Papadakis and Tsimas, 2002; Qaidi et al., 2022; Rakhimov et al., 2017; Sobol et al., 2015; Tayeh et al., 2022; Wasim et al., 2022; Xia et al., 2021). Both pumice pozzolan and pozzolan extracted from quarry aggregate are considered strong candidates in this group of SCM for producing cement, mortars, and concretes. The use of pozzolans as partial replacements for cement leads to a reduction in $CO_2$ emissions, as the cement industry is the third largest producer of $CO_2$ in the world, behind only energy production and transport (Amran et al., 2022; Abiodun et al., 2022; Fan and Miller, 2018; International Energy Agency, 2024; Miller et al., 2016; Nature, 2021; Neupane, 2022; Tayeh et al., 2022). Reducing emissions from cement production is difficult due to the current reliance on carbon-containing raw materials and high-temperature heating requirements (Summerbell et al., 2016). Energy efficiency (Moumin et al., 2020), materials (Barcelo et al., 2014; Sammer et al., 2024) and low-emission fuels (Zhang and Mabee, 2016) are key short-term measures. Deeper reductions require massive deployment of innovative technologies, such as cements made from alternative raw materials and Carbon Capture Solutions (CCUs) (Report International Energy Agency (IEA), 2023).

The effect of adding pozzolan to mortars and concretes depends on various factors, including the type of pozzolan and the percentage of cement or aggregate replaced. These additions often result in increased durability (Çavdar and Yetgin, 2007; Dedeloudis et al., 2018; Hunyak et al., 2019; Kushnir et al., 2021; Markiv et al., 2016; Mertens et al., 2009; Papadakis and Tsimas, 2002; Rojas and Cabrera, 2002; Shi, 1998; Sobol et al., 2015; Tayeh et al., 2022; Xia et al., 2021; Zhang and Malhotra, 1995), decreased heat of hydration (Najimi et al., 2008; Shi, 1998), enhanced resistance to sulfate attack (Janotka and Krajči, 2003; Najimi et al., 2008), prolonged setting time, prevention of water penetration (Ahmadi and Shekarchi, 2010; Janotka and Krajči, 2003; Najimi et al., 2008), and reduced energy cost per unit of cement (Rojas and Cabrera, 2002). The origin of this activity lies in the nature and quantity of silica-based materials it contains and is further enhanced with an increase in the disorder of its crystalline structure (Türkmenoğlu and Tankut, 2002). The siliceous and aluminous materials present in tuffs affect their pozzolanic activities significantly. Quartz, feldspar, mica, hornblende, pyroxene, zeolites, cristobalite, clay minerals, amorphous pumice, and glass shards can be combined in tuffs. In general, a good pozzolanic tuff has low quantities of clay minerals, low quantities of

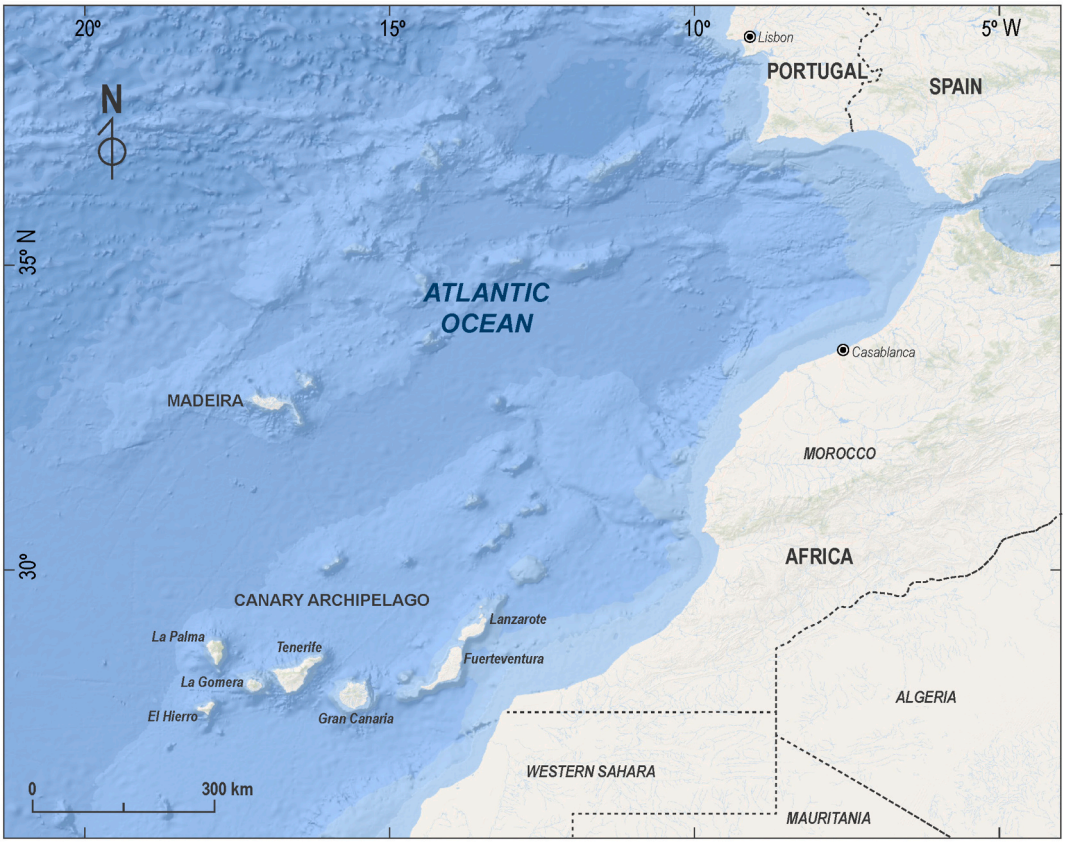


**Fig. 1.** Geographical location of the Canary Archipelago.

alkali feldspar, high quantities of zeolite minerals, and volcanic glass. In addition, it should exhibit high porosity and specific surface area.

The Canary Islands, located northwest of the African continent, approximately 100 km from the Saharan coast (Fig. 1), form an oceanic archipelago that originated from predominantly alkaline intraplate volcanism (Ahmadi and Shekarchi, 2010). The age of the Canary archipelago dates back to the lower-middle Miocene, 20 million years ago, when the first manifestations of subaerial volcanism began (Ancochea et al., 1990; Coello et al., 1992). Fractional crystallization processes caused the magmas to change from basic terms (basalt, basanite, tephrite) to salic (trachytes and phonolites), resulting in eruptions that released these latter materials mainly in the central islands (Tenerife and Gran Canaria). As a result, the igneous rocks of the islands probably encompass the widest spectrum of chemical composition and mineralogy known in any intraplate oceanic system (Schmincke and Sumita, 2010). Thus, the variety of formations, products, and volcanic lithologies present make this archipelago to be considered one of the best and most complete natural volcanological laboratories in the world.

This study characterizes pozzolans from volcanic quarries located in the Canary Islands and evaluates their suitability as cement substitutes in mortars with basaltic aggregates. Their physical, chemical, geochemical, mineralogical, and pozzolanic properties were analyzed, and their reactivity was evaluated in comparison with other materials such as filler or silica fume. Parameters characteristic of cement pastes and mortars specimens were also determined. We also quantify the cradle-to-gate $CO_2$ implications of clinker substitution to align the material performance with sustainability outcomes (Hernández González and Barbero Barrera, 2023). Unlike previous studies that address volcanic pozzolans mainly from a purely mechanical or generic environmental perspective (Santana et al., 2022; Presa et al., 2023), the present work establishes an integrated framework linking detailed geological characterization, standardized masonry mechanical performance, and performance-normalized $CO_2$ reduction using locally sourced volcanic resources from an insular territory. This integrated approach provides a transferable methodology that can be extrapolated to other volcanic regions worldwide as a practical strategy to support low-carbon cement production (Barbhuiya et al., 2024).

## 2. Materials and methods

### 2.1. Materials

Two existing pozzolans, namely tuff (PZT) and quarry (PZQ) pozzolans and the polishing powder (PP) generated in the manufacturing of mortars and concrete were investigated as potential substitutes for cement. Pozzolanic tuff (PZT) was obtained from the crushing and grinding of the rock classified as the lithotype of unwelded ignimbrite (NWIG) (Hernández Gutiérrez, 2014) from a representative commercial block of tuff from the island of Tenerife (Canary Islands, Spain) (Santana et al., 2022). The quarry pozzolan (PZQ) comes from the quarry dismantling. It is a fine powder with a true density or specific weight of 2550 kg/m$^3$, produced as a waste material during the extraction process, in search of optimal aggregate extraction layers. The polishing powder (PP) is a concrete residue generated by polishing the top surface of concrete specimens and has a true density of 2680 kg/m$^3$. As a reference element chosen to evaluate the behavior of the previous materials in mortar mixtures, silica fume (SF) was selected. The SF used was Techmo Fume SD-92 (Técnicas de Hormigón y Morteros S.L., Las Palmas de Gran Canaria, Spain). Fig. 2 shows the granulometric analysis of the materials.

Mortar specimens were fabricated in accordance with the standard UNE EN 1015-11 (AENOR, 2020) using CEM IV/B-P/32.5N and CEM II/A-P/42.5R/MR from Cemento Teide (Votorantim Cimentos, Santa Cruz de Tenerife, Spain). CEM I/42.5R/SR was used as the reference cement for the pozzolanic activity tests and compressive strength tests at 28 days, in accordance with the UNE 80303–2:2017 (AENOR, 2017) and

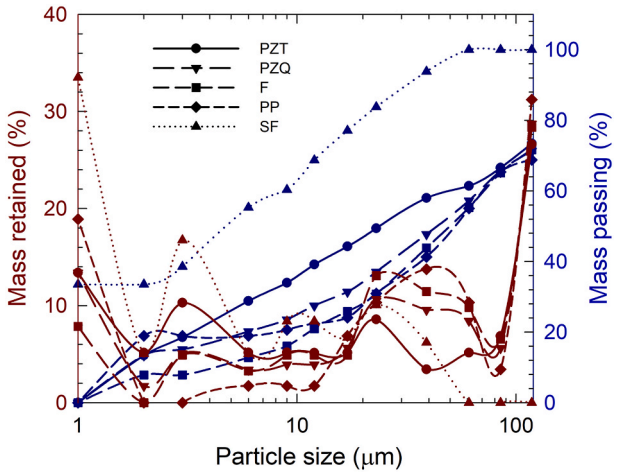


**Fig. 2.** Granulometric analysis of filler (F), silica fume (SF), polishing powder (PP), tuff pozzolan (PZT) and quarry pozzolan (PZQ), wet sieving.

UNE-EN 196-1 (AENOR, 2018a) standards. Physical, chemical and mechanical properties, and relevant standard limit values of these cements are given in Table 1.

The aggregates used in both mortars are obtained from crushing basaltic rocks, generally classified as MAB lithotype (massive aphanitic basalt) (Hernández Gutiérrez, 2014). Given the volcanic nature of our aggregates, mortar samples were prepared using bagged basaltic sand 0/4 mm sieved to 0/2 mm (BS) and a standardized sand with AENOR certification (SS). This allows us to understand the extent to which the nature of our Canary Islands aggregate type affects mortar formulations. The main properties of the aggregates are shown in Table 2.

#### 2.1.1. Cement pastes

Six samples of cement paste (C) were prepared using four types of cement (CEM IV/B-P/32.5N; BL I 52.5R; CEM II/A-P/52.5R; and CEM II/A-P/42.5R), following the UNE-EN 196-3 (AENOR, 2017b) standard, with dosages and codes detailed in Table 3. For each cement type, the water/cement ratio (w/c) was adjusted to achieve three target 28-day compressive strength levels (approximately 54, 65 and 74 N/mm$^2$). This setup yields pairs of mixtures with similar compressive strength but different cement types (see Table 3), thus distinguishing the influence of cement composition from the mere effect of strength level or water content and paste porosity. The samples were tested according to UNE-EN 197-1 (AENOR, 2011a) and UNE-EN 196-1 (AENOR, 2018a), which establish the testing methods and usage specifications.

**Table 1**
Chemical, physical and mechanical properties of cements IV/B-P/32.5N and II/A-P/42.5R/MR. CEM I/42.5R/SR was used as the reference cement.

| | CEM IV/B-P/32.5N[a] | CEM II/A-P/42.5R/MR[a] | CEM I/42.5R/SR[a] |
|---|---|---|---|
| Loss on ignition (LOI) | 5.7 | 3.4 | 3.0 |
| Insoluble residue (IR) | 20.1 | 10.1 | 1.9 |
| Chloride ($Cl^-$, %) | 0.02 | 0.01 | >0.1 |
| Sulfates ($SO_3$, %) | 2.91 | 3.38 | 3.2 |
| Initial setting time (min) | 190 | 150 | 190 |
| Pozzolan content (%) | 41 | 19 | – |
| Clinker content (%) | 54 | 76 | 95 |
| Gypsum content (%) | 5 | 5 | 5 |
| End of hardening (FEH, min) | 250 | 215 | – |
| Expansion (Le Chatelier EXP, mm) | 1.0 | 0.0 | 0.5 |
| Compressive strength at 7 days (N/mm$^2$) | 25.1 | 37.0 | 30.5 |
| Compressive strength at 28 days (N/mm$^2$) | 37.2 | 51.6 | 53.3 |

[a] Data provided by the Manufacturer.

**Table 2**
Characterization of the aggregates according to European Union (EU) standards.

| | | Sand 0/4 mm | Coarse 10/20 mm |
|---|---|---|---|
| Sand equivalent (AENOR, 2000) | | 67 | – |
| Grain size distribution and fines content (%) (AENOR, 2012a) | | 7–10 | – |
| Flakiness index (AENOR, 2012b) | | – | 7.1 |
| Relative density of coarse and fine aggregate ($g/cm^3$) (AENOR, 2025) | $\delta_a$ | 2.85 | 2.8 |
| | $\delta_{rd}$ | 2.6 | 2.53 |
| | $\delta_{rds}$ | 2.69 | 2.64 |
| Absorption of coarse and fine aggregate (%) (AENOR, 2025) | | 3.97 | 3.65 |
| Chloride content (AENOR, 2010) | | $1.7 \times 10^{-3}$ | $3.5 \times 10^{-4}$ |
| Content of water- and acid-soluble sulfates (AENOR, 2010) | | no | no |
| Total sulfur content (AENOR, 2010) | | no | no |
| Light organic pollutants (AENOR, 2010) | | $6.6 \times 10^{-2}$ | – |
| Humus content (sand) (AENOR, 2010) | | More clear | – |

**Table 3**
Identification, classification, and characteristics of cement paste samples.

| Code | Cement type | Water/cement ratio (w/c) | Compressive strength at 28 days ($N/mm^2$) |
|---|---|---|---|
| C1 | CEM IV/B-P/32.5R | 0.34 | 74.1 |
| C2 | BL I 52.5R | 0.32 | 53.7 |
| C3 | BL I 52.5R | 0.40 | 65.0 |
| C4 | CEM II/A-P/52.5R | 0.32 | 74.1 |
| C5 | CEM II/A-P/42.5R | 0.41 | 53.7 |
| C6 | CEM IV/B-P/32.5N | 0.26 | 65.0 |

### 2.1.2. Mortars

Samples of mortar were prepared to investigate, through preliminary tests before the production of concrete, the influence of aggregate type, cement type, and a variety of additives that can substitute up to 20 % of cement. The two most commonly used types of cement in the Canary Islands were used: Portland cement (CEM II/A-P/42.5R) and pozzolanic cement (CEM IV/B-P/32.5N). As for the different types of additives, they were used to replace 20 % of the cement, aiming to detect potential improvements compared to a standard mortar without additives. The additives used were filler (F), volcanic tuff pozzolan (PZT), and silica fume (SF). The filler (F) is a quarry byproduct from aggregate crushing, with a density of 2700 $kg/m^3$. It consists of rock dust generated by friction between the different particles as they are crushed to the target sizes in the quarry, typically gravel and sand with particle size distributions between 20 and 0.063 mm. This process leaves a residue with particle sizes smaller than 0.063 mm, which the quarry or concrete and asphalt producer must remove, incurring an associated cost. Silica fume (SF) SD-92 (Techmo, Agüimes, Spain) was used as an additive. It consists of very fine spherical particles containing a high proportion (82–96 %) of amorphous silica ($SiO_2$), with a density of 2200 $kg/m^3$.

For the tests, 16 mortar specimens of size 4 cm × 4 cm x 16 cm were prepared according to standard UNE-EN 1015-11 (AENOR, 2020), which specifies the procedure for the preparation and curing masonry mortars. The mortars were prepared using a mass ratio of one part cement to three parts sand, with a water/cement ratio of 0.50, following the general formulation criteria commonly adopted for standardized mortar mixtures. Table 4 shows the composition and coding of the samples. All specimens were cured in a moist chamber until reaching 28 days, following standard UNE-EN 196-1 (AENOR, 2018a). After this period, they underwent tests for flexural and compressive strength.

**Table 4**
Coding, classification and characteristics of the tested mortar samples. Code: M1 = CEM II/A-P/42.5R cement; M2 = CEM IV/A-P/32.5N cement; SS = Standard Sand; BS = Bagged Sand; P = Without substitution; PZT = Pozzolanic tuff; F = filler; SF = silica fume.

| Code | Cement | Sand | Additions |
|---|---|---|---|
| M1SSP | CEM II/A-P/42.5R | Standard sand | Without substitution |
| M2SSP | CEM IV/A-P/32.5N | | Without substitution |
| M1SSPZT | CEM II/A-P/42.5R | | Pozzolanic tuff |
| M2SSPZT | CEM IV/A-P/32.5N | | Pozzolanic tuff |
| M1SSF | CEM II/A-P/42.5R | | Filler |
| M2SSF | CEM IV/A-P/32.5N | | Filler |
| M1SSSF | CEM II/A-P/42.5R | | Silica fume |
| M2SSSF | CEM IV/A-P/32.5N | | Silica fume |
| M1BSP | CEM II/A-P/42.5R | Bagged sand | Without substitution |
| M2BSP | CEM IV/A-P/32.5N | | Without substitution |
| M1BSPZT | CEM II/A-P/42.5R | | Pozzolanic tuff |
| M2BSPZT | CEM IV/A-P/32.5N | | Pozzolanic tuff |
| M1BSF | CEM II/A-P/42.5R | | Filler |
| M2BSF | CEM IV/A-P/32.5N | | Filler |
| M1BSSF | CEM II/A-P/42.5R | | Silica fume |
| M2BSSF | CEM IV/A-P/32.5N | | Silica fume |

### 2.2. Experimental methods

The mineralogical and petrographic properties of the samples were identified under a polarized light microscope using thin sections prepared with a petrographic microscope model Labophot2 Pol (Nikon, Shinagawa, Japan). The X-ray diffraction (XRD) analysis of the bulk powder samples was conducted using a D8 ADVANCE XRD X-ray diffractometer (Bruker™, Karlsruhe, Germany). For the purpose of the study, a CuK radiation (1.5406 Å) with a step size of 0.02°, a power of 45 kV, and a current of 40 mA, in the range of $2\theta$ = 20–100 was employed. The micromorphological characteristics of the tuffs were examined using a JEOL-JSM-6400 scanning microscope using an accelerating voltage of 20 kV and a working distance of 39 mm (Akishima, Tokyo, Japan). An energy-dispersive X-ray spectrometer (EDX) FESEM Zeiss Sigma 300VP was used for elemental analysis (Zeiss, Oberkochen, Germany), and Zeiss SmartEDX software version 1.5 was employed for data processing.

The major elemental analysis of the samples, including $Co_3O_4$, CuO, NiO, $SiO_2$, $TiO_2$, $Al_2O_3$, $Fe_2O_3$ total, MnO, MgO, CaO, $Na_2O$, $K_2O$, $P_2O_5$, $Cr_2O_3$, $V_2O_5$ and $SO_3$, was conducted using Fusion X-ray Fluorescence (XRF) Analysis (XRF Whole Rock Package). $CO_2$ and $SO_4^{2-}$ were determined using infrared analysis, and $Cl^-$ was analyzed using Short Lived Instrumental Neutron Activation Analysis (INAA). Loss on Ignition (LOI) was determined gravimetrically. All these analyses were performed by Activation Laboratories Ltd. (Actlabs), headquartered in Ancaster, Ontario, Canada (LabID 266).

All additives used in the mixtures were assessed to determine the pozzolanic activity index (IAP) with lime according to ASTM C 311 (ASTM, 2013) and specified in UNE 80303-2 (AENOR, 2017a), section 7.2.b), and following the test method UNE-EN 196-5 (AENOR, 2011b) at 7 days. The reference cement used was Type I/42.5R/SR, which was blended with each additive in a cement/additive ratio of 75/25 (75 % cement and 25 % additive by mass), as prescribed in UNE 80303-2 for the evaluation of pozzolanic additions. This mixture (20 g) was hydrated with 100 mL of water. The result is determined by comparing the amount of calcium hydroxide present after a fixed period of 7 days at a temperature of 40 °C.

The tests conducted include flexural and compressive strength at 28 days for mortars according to UNE-EN 1015-11 (AENOR, 2020) and they were performed using a 1-tonne universal press model SAL-1Tn (Salmer, Valencia, Spain), and a 12-tonne cement press model HDR120KN (Hidrensa, Madrid, Spain), respectively.

### 2.3. Life-cycle assessment (cradle-to-gate) – method

A simplified cradle-to-gate life-cycle assessment (LCA) was conducted on a functional unit of 1 tonne of binder (cement + SCM). The environmental assessment was performed through a $CO_2$ calculation model based on a spreadsheet-based developed by the authors, based exclusively on emission factors reported in the literature and official energy and electricity statistics, without the use of commercial LCA software or proprietary databases. System boundaries included clinker production, cement milling/blending, SCM extraction (when applicable), SCM grinding, and truck transport. The baseline scenario assumed 80 % clinker in cement; the scenario assessed a 20 % clinker substitution with volcanic SCMs. Transport distances were set to 40 km for SCM and 50 km for clinker.

Emission factors for clinker production, diesel consumption for transport, grinding energy demand, and the regional electricity generation mixes were obtained from peer-reviewed literature and official government sources. All numerical values used in the calculations are explicitly reported and analyzed in Section 3.5. Performance-normalized environmental indicators (kg $CO_2$/(MPa·m$^3$)) were also calculated based on the 28-day compressive strength data and the typical binder content in the mortar.

For quarry waste used as SCMs, a cut-off allocation was applied to exclude extraction costs and account only for the impacts of processing and transport. This methodological approach is consistent with the principles of the circular economy principles and the valorization of industrial by-products.

## 3. Results and discussion

### 3.1. Geochemical classification of materials in the Canary Islands

First, a geochemical classification of the samples that can be found in the Canary Archipelago was made in terms of their Total Alkali Silica (TAS) by using the analytical information reported by Rodríguez-Losada et al. (2009) and Hernández et al. (2011) on 265 samples from the entire Canary archipelago. In this way, the TAS geochemical classification given in Fig. 3 was created, which relates the content of alkaline minerals ($Na_2O$ and $K_2O$) and the content of silicates ($SiO_2$) (Le Maitre et al., 2002). It can be observed that the volcanic rocks present in the Canary Islands cover almost the entire diagram, except for the Andesite group.

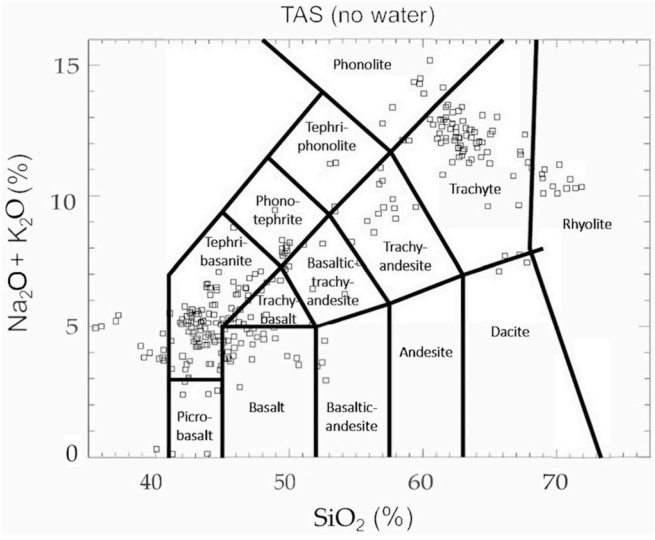


**Fig. 3.** Total Alkali Silica (TAS) geochemical classification of over 265 rocks in the Canary Islands sampled by Rodríguez-Losada et al. (Rodríguez-Losada et al., 2009) and Hernández et al. (Hernández et al., 2011).

Among all these rocks, considering their geochemical composition, those potentially useable as pozzolans for cement manufacturing are the phonolite, trachyte, and rhyolite associated with loose granular pyroclastic deposits or soft rocks. These deposits are mainly found in the central islands of Tenerife and Gran Canaria (Fig. 4a and b).

On the island of Tenerife, these pyroclastic deposits belong to the geological unit of the Cañadas Edifice and are identified as undifferentiated salic pyroclasts (Barrera Morate and García Moral, 2011). They date from between 0.54 and 0.15 Ma (Upper Pleistocene). They mainly outcrop on the southern and southeastern slopes of the island and once covered almost the entire area. Their soft material nature has facilitated the development of a significant network of ravines and streams, dividing these deposits into numerous outcrops. These deposits are not homogeneous as they include pyroclasts of different nature and texture. They exhibit varying degrees of compaction, with the common denominator being the predominance of pumice. Although the exact emission centers are not known, it is inferred that there must have been many, located in the central part of the island, where the Caldera de Las Cañadas and El Teide are currently found.

The salic pyroclastic deposits of Gran Canaria belong to the island's First Volcanic Cycle, which occurred between 14 and 9 Ma and includes a wide variety of materials with different compactness and textures. This cycle began with the rapid emission of a large amount of basaltic lavas, followed by differentiation in the magma chamber that produced significant volumes of salic materials (trachytes and rhyolites). These emissions caused the collapse of the chamber and the formation of the Tejeda Caldera (Hernán, 1976; Schmincke, 1967). As a result, large volumes of salic pyroclastic flows formed and occupied the southwestern part of the island (Fig. 4b). Among all the materials emitted during this volcanic cycle, the Miocene pozzolans of the Fataga Formation, dating to the Upper Miocene around 10.4 Ma, are particularly notable. These are slightly welded ash and pumice ignimbrites that have been exploited for decades for cement manufacturing.

In addition to geochemical composition, an important factor for the utilization of rocks as pozzolanic material is their physico-mechanical properties, primarily density and uniaxial compressive strength. For environmental ($CO_2$ emissions) and economic considerations, less dense and softer rocks are preferred for obtaining pozzolans through rock crushing and grinding. Otherwise, energy, machinery, and production time costs would increase substantially. Hernández-Gutiérrez (Hernández Gutiérrez, 2014) proposed a simplified classification of Canary volcanic rocks for their application in civil engineering and architecture, categorizing them into 10 lithotypes based on their geochemical and physico-mechanical properties (Table 5).

Among these lithotypes, those with trachytic, phonolitic, and rhyolitic composition are: TRC, PHN, WIG, and NWIG. The lithotypes TRC, PHN, and WIG correspond to very hard and cohesive rocks, with high average values of apparent density and uniaxial compressive strength (UCS): TRC has an apparent density of 23.9 kN/m$^3$ and UCS of 95.5 MPa; PHN has an apparent density of 24.3 kN/m$^3$ and UCS of 118.9 MPa; WIG has an apparent density of 20.9 kN/m$^3$ and UCS of 48.2 MPa. However, the NWIG lithotype is characterized by much lower values of apparent density (15.7 kN/m$^3$ on average) and UCS (16.5 MPa on average). The NWIG lithotype is very abundant in the central islands of Gran Canaria and Tenerife (cf. Fig. 4).

In addition to NWIG, the granular, loose, or low-compactness pyroclastic deposits are also of great interest. Among them, materials with pozzolanic properties include pumice (of trachytic, phonolitic, or rhyolitic composition), which is a granular material (see Fig. 5) with high porosity, light weight (densities between 4 and 9 kN/m$^3$), easily friable, effective as a thermal insulator, and easy to extract in open-pit quarries.

The pumice deposits, like the NWIG, are found on the islands of Tenerife and Gran Canaria, where highly explosive, salic-type eruptions occurred. These eruptions produced large eruptive columns reaching kilometer heights, which were pushed by the north-component trade

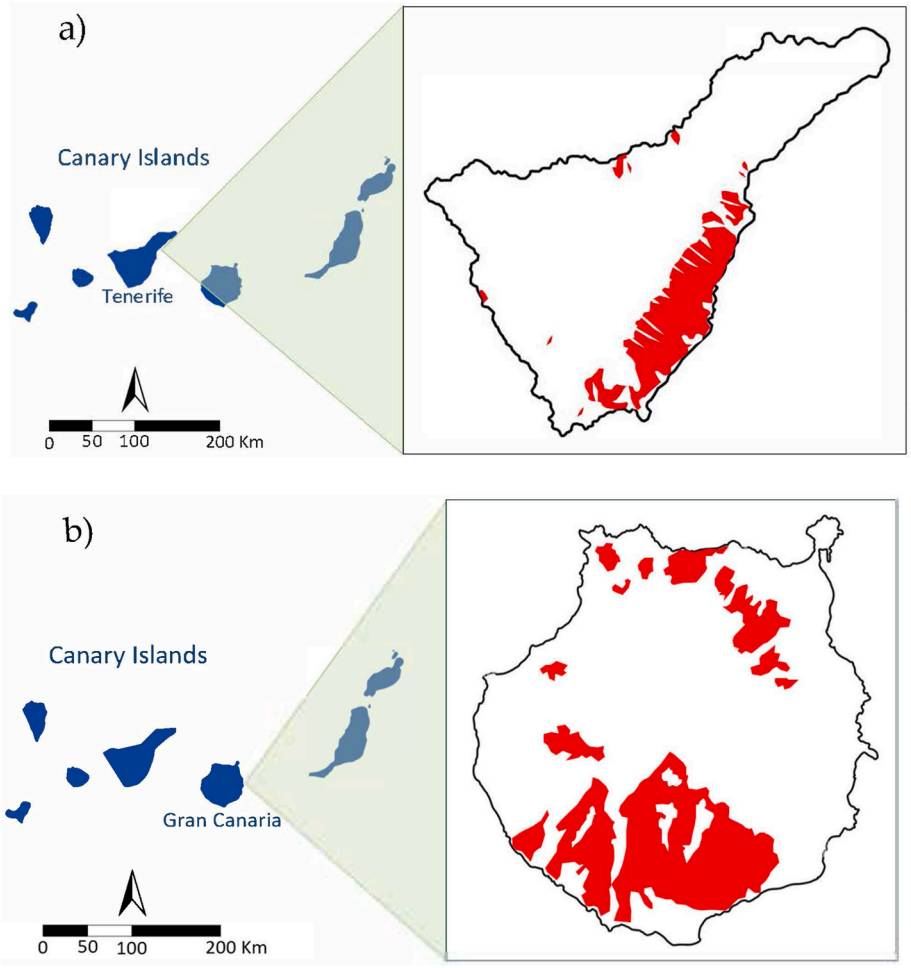


**Fig. 4.** Geographical distribution of pyroclastic deposits with trachytic, phonolitic, and rhyolitic compositions on the islands of Tenerife (a) and Gran Canaria (b).

**Table 5**
Classification of lithotypes of the Canary Islands according to their geochemical and physico-mechanical properties.

| | | | |
|---|---|---|---|
| Basalt (B) | Aphanitic (AB) | Massive (M) | MAB |
| | | Vacuolar (V) | VAB |
| | Olivinic-Pyroxenic (OPB) | Massive (M) | MOPB |
| | | Vacuolar (V) | VOPB |
| | Plagioclasic (PB) | Massive (M) | MPB |
| | | Vacuolar (V) | VPB |
| Trachyte (TRC) | | | TRC |
| Phonolite (PHN) | | | PHN |
| Ignimbrite (IG) | Welded (W) | | WIG |
| | Non-welded (NW) | | NWIG |

winds, causing them to collapse towards the southern slopes of both islands. For this reason, the main deposits of pozzolanic materials are located in the south of these islands (Alonso Blanco, 1989). Both NWIG and pumice are generated in the same eruptive process, so it is common for them to appear in overlapping layers within the same outcrop.

**Fig. 5.** Detail of an outcrop of fall deposits of salic pyroclasts (pumice).

### 3.2. Petrographic analysis by thin-sections (PATS)

#### 3.2.1. MAB lithotypes

On the island of Tenerife, aggregates (sand and gravel) used in both mortars and concretes primarily come from the crushing of basaltic rocks, generally classified as MAB (massive aphanitic basalt) lithotypes (Hernández Gutiérrez, 2014). Table 6 summarizes some of geo-mechanical characteristics of this rock, whereas Fig. 6 shows a thin-section image of this lithotype. A homogeneous cryptocrystalline mass is observed, lacking vacuoles, with a texture formed by tiny crystals whose crystalline nature is not observable under a microscope. It also includes a microcrystalline texture (small crystals only visible under a microscope) composed of microlites of olivine (iddingsitized or not), augite, plagioclase, and opaque metallic minerals. From a lithological perspective, it is a basaltic rock with an aphanitic texture (without visible crystals), typically light gray in color, with a planar fabric that is

**Table 6**
Petrological and geomechanical characteristics, and X-Ray Fluorescence (XRF) analysis, of the massive aphanitic basalt (MAB) lithotype and the non-welded gnimbrite (NWIG) rock.

| Determination of the specific weight of the rock (kg/m$^3$) | MAB | NWIG |
|---|---|---|
| Apparent | 2840 | 2200 |
| Dry | 2730 | 1640 |
| Saturated | 2770 | 1900 |
| Real solid particles | 2910 | 2210 |
| Porosity (%) | | |
| Total | 5.54 | 44.4 |
| Open | 3.59 | 22.6 |
| Absorption (%) | 1.23 | 5.98 |
| Compressive strength (MPa) | 104.4 | 16.5 |

| X-Ray Fluorescence (XRF) analysis (%) | $SiO_2$ | $Al_2O_3$ | $Fe_2O_3$ | CaO | MgO | $Na_2O$ | $K_2O$ | MnO | $P_2O_5$ | $TiO_2$ | LOI | $SO_4^{2-}$ | $Cl^-$ |
|---|---|---|---|---|---|---|---|---|---|---|---|---|---|
| MAB | 44.11 | 15.02 | 14.9 | 9.47 | 6.31 | 4.01 | 1.26 | 0.204 | 0.80 | 4.53 | 0.71 | <0.05 | 0.19 |
| NWIG | 50.19 | 17.35 | 3.08 | 1.45 | 1.31 | 6.42 | 4.94 | 0.15 | 0.10 | 0.64 | 14.38 | 0.21 | 0.53 |

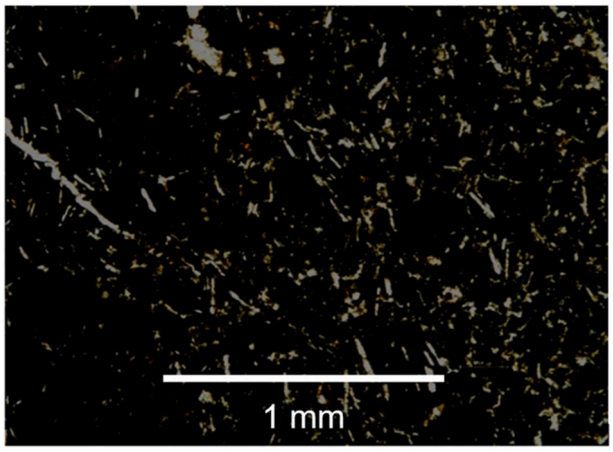


**Fig. 6.** Thin-section image taken with unpolarized light of the massive aphanitic basalt (MAB) lithotype used in the study. It corresponds to the basaltic aggregate, coded (A), used in the mixtures.

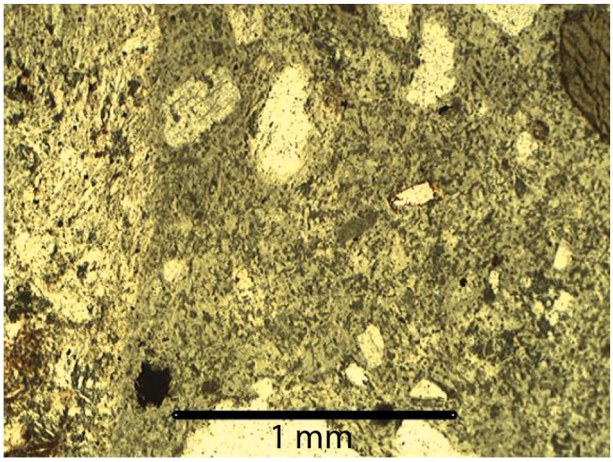


**Fig. 7.** Thin-section image taken with unpolarized light of the non-welded ignimbrite (NWIG) lithotype used in the study.

occasionally marked by the presence of small, laterally discontinuous joints. Although classified as massive, it can exhibit dispersed vesicles with an average size of 2–3 mm. Outcrops are generally found in "aa" basaltic flows with a central zone of hard rock featuring cooling-induced contraction joints, bordered above and below by scoria levels (granular material with little or no cohesion).

### 3.2.2. NWIG lithotypes

Table 6 gives the geomechanical characteristics of the rock and Fig. 7 shows a thin-section obtained under the petrographic microscope using unanalyzed polarized light. It can be seen that the PZT consists of a chaotic mixture of pumice fragments (1–4 cm), ash, rock fragments, and crystals. They present an abundant light yellow cineritical matrix. The typical outcrops of these rocks correspond to relatively thick layers of massive rock, with few or no joints, low density, and low uniaxial compressive strength (see Fig. 5). A trachytic or phonolitic composition is found, and under the petrographic microscope, crystals of anorthoclase or sanidine, irregularly shaped glass fragments, aegirine fragments, hornblende, and opaque minerals can be observed, all in a microcrystalline or glassy matrix.

## 3.3. Structural, morphological and compositional analysis

Fig. 8 shows the X-ray diffraction (XRD) patterns obtained from the PZT, PZQ and PP samples. From an analysis of the results obtained, it is observed that the PZT sample presents merlinoite ($K_5Ca_2(Al_9Si_{23}O_{64})\cdot 24H_2O$), sanidine ($(Na,K)(Si_3Al)O_8$), potassium magnesium silicate ($K_{1.14}Mg_{0.57}Si_{1.43}O_4$Mg-BCTT), silicon oxide ($SiO_2$), biotite ($(K,Na)(Mg,Fe,Ti)_3(Si,Al)_4O_{10}(OH,O)_2$), gypsum ($CaSO_4\cdot 2H_2O$) and amorphous phase. By groups, the composition is zeolites 27.30 %, plagioclase 49.45 %, quartz 16.38 %, biotite 5.40 %, and gypsum 1.46 %. PZQ sample presents phillipsite-K ($(K_2)_{0.48}CaO_{0.52}Al_2Si_4O_{12}\cdot xH_2O$), albite ($(Na,Ca)Al(Si,Al)_3O_8$), diopside ($Ca(Mg,Al)(Si,Al)_2O_6$), clinotobermorite ($Ca_5Si_6(O,OH,F)_{17}\cdot 5H_2O$), merlinoite, sanidine, biotite, quartz ($SiO_2$), and amorphous phase. By groups, the composition is zeolite 21.42 %, plagioclase 44.15 %, biotite 6.61 %, quartz 2.90 %, and piroxene 24.92 %. PP sample presents phillipsite-K, anorthite ($CaAl_2Si_2O_8$), albite, merlinoite, sanidine, quartz, diopside, clinotobermorite and amorphous phase. By groups, the composition is zeolite 11.93 %, plagioclase 67.5 %, quartz 2.29 %, and piroxene 18.28 %.

In Fig. 9, SEM images obtained for the four samples are displayed whereas Fig. 10 shows EDX analysis diagrams obtained from the SEM micrographs in Fig. 9. Although the SEM-EDX graphs reveal the complex microstructure of the natural pozzolans, it must be noticed that the SEM-EDX data are in agreement with the information provided by XRD. For the PP, PZT, and PZQ samples, the predominant presence of larger plagioclase grains is observed, along with dispersed zeolite fibers throughout the matrix (Türkmenoğlu and Tankut, 2002).

Major elemental oxide compositions of tuff samples obtained using XRF analysis are shown in Table 7 and reflect their mineralogical characteristics, highlighting that $Co_3O_4 \leq 0.005$ %, CuO $\leq 0.005$ %, NiO $\leq 0.003$ %, $Cr_2O_3 \leq 0.01$ %. Abnormally high CaO contents (19.37 %) and LOI (11.27 %) values are found for sample PP and a high LOI (14.96

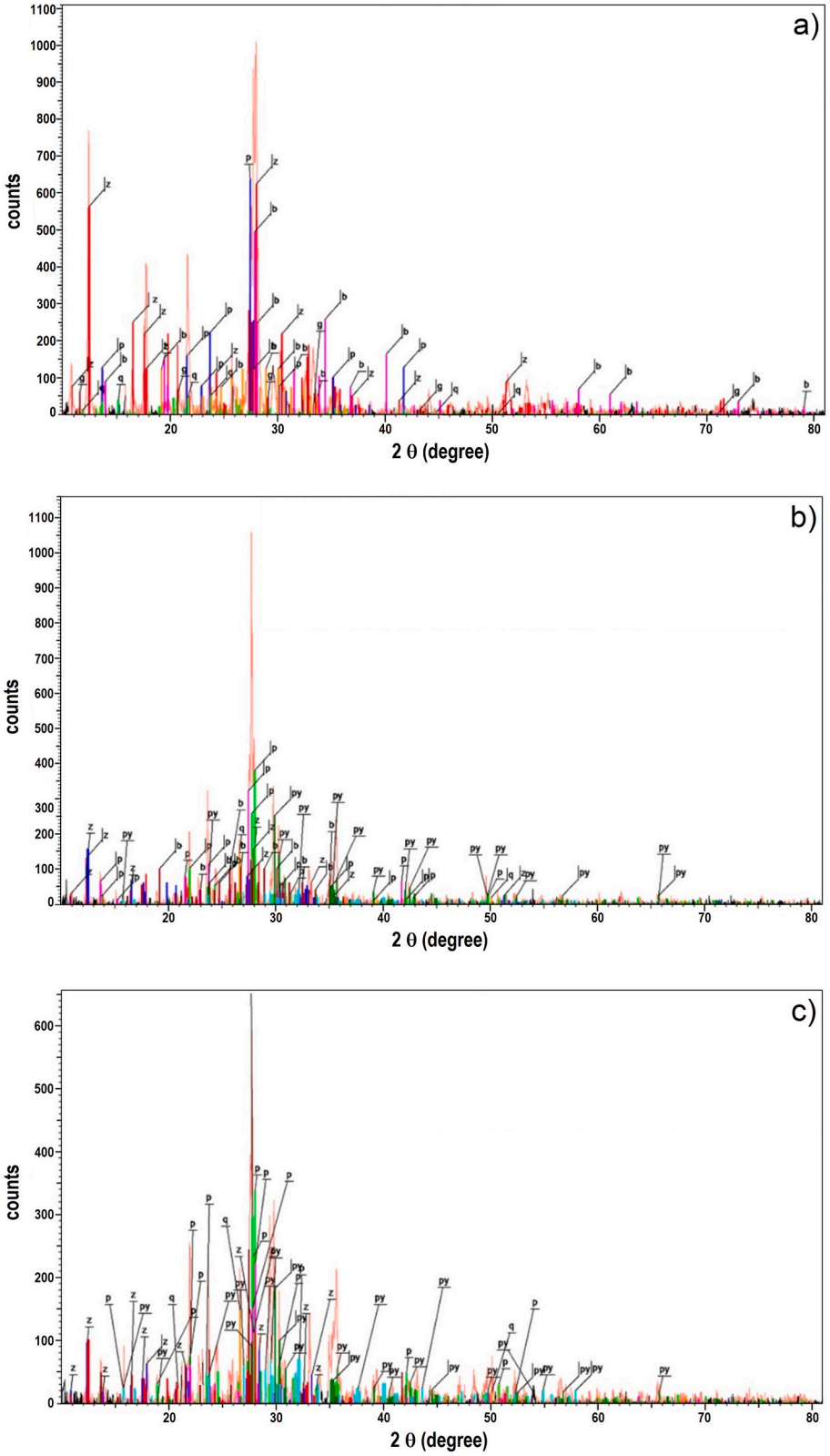


**Fig. 8.** XRD patterns obtained from the addition materials: (a) puzzolan tuff (PZT), (b) puzzolan quarry (PZQ), and (c) polishing powder (PP) samples. Legend: *z*, zeolites (merlinoite and phillipsite-K); *p*, plagioclases (sanidine, albite and anorthite); *q*, silicon oxide; *b*, biotite; *g*, gypsum; and *py*, piroxenes (diopside and clinotobermorite). (For interpretation of the references to color in this figure legend, the reader is referred to the Web version of this article.)

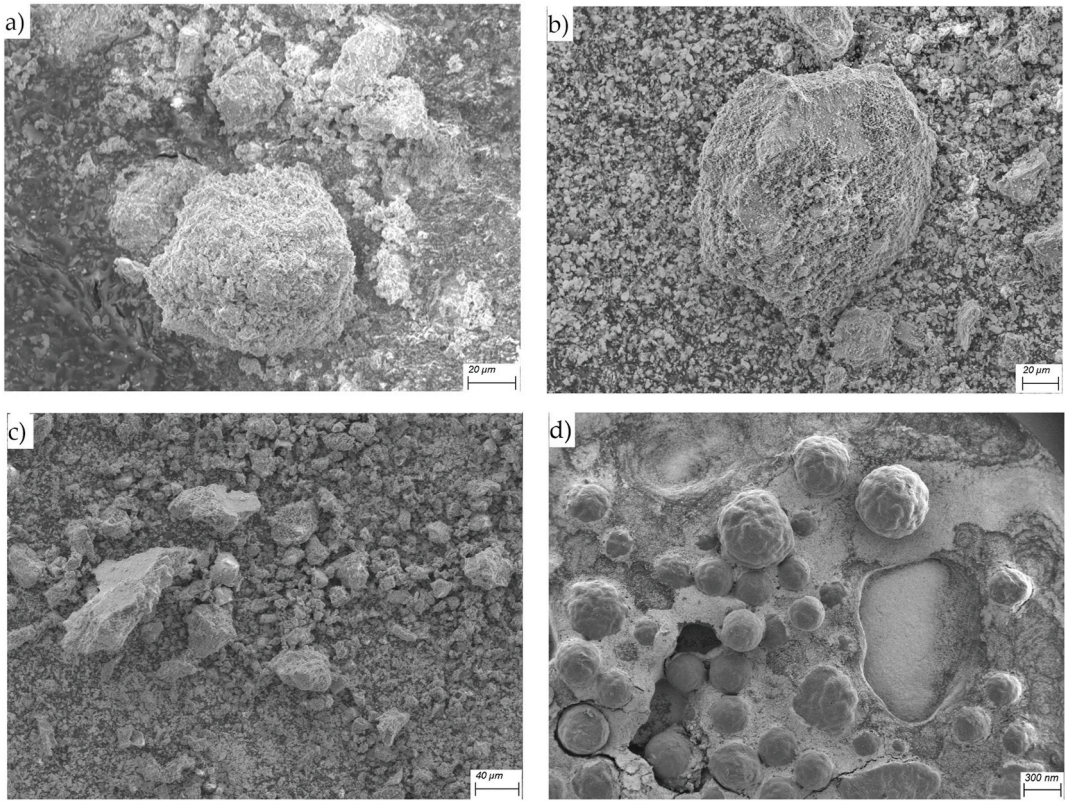


**Fig. 9.** Typical SEM images showing the morphology of the additions considered in this work: a) pozzolanic tuff (PZT), b) pozzolanic quarry (PZQ), c) polishing powder (PP), and d) silica fume (SF).

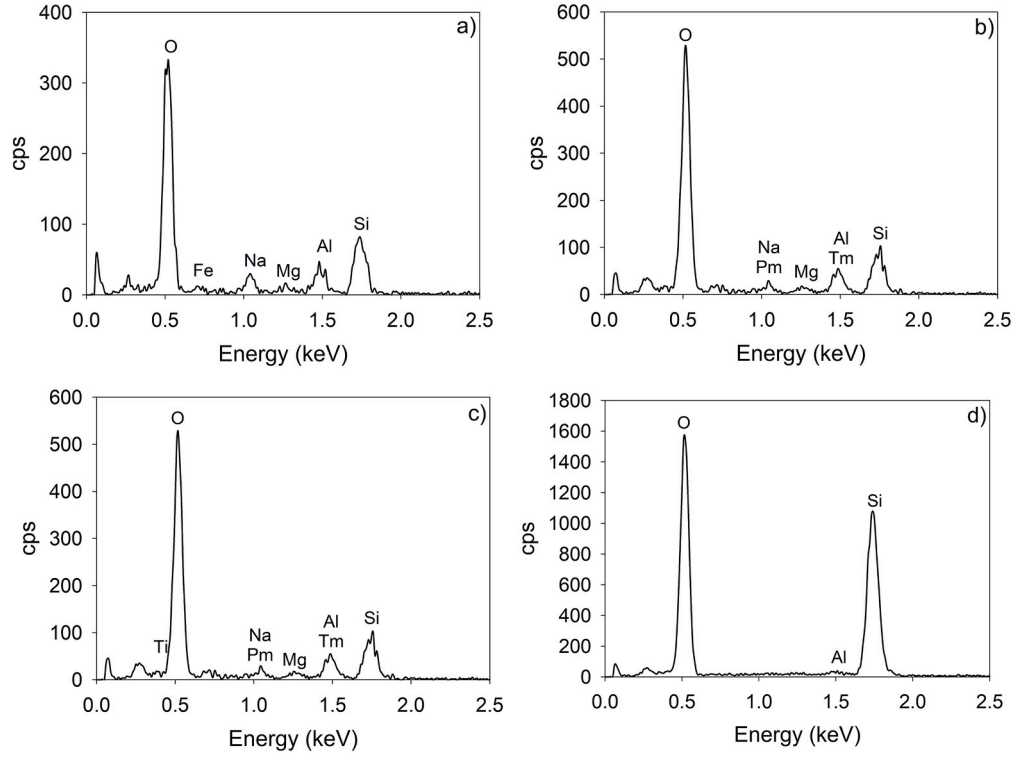


**Fig. 10.** EDX analysis of the microstructure of the additions shown in Fig. 9: a) pozzolanic tuff (PZT), b) pozzolanic quarry (PZQ), c) polishing powder (PP), and d) silica fume (SF).

%) value for sample PZT. $SiO_2$ values vary between 37.58 % and 91.80 % and $Al_2O_3$ between 0.59 % and 16.72 %. The results of the chemical

**Table 7**
X-Ray Fluorescence (XRF) analysis and reactivity of the additions (in %).

| Code | $SiO_2$ | $Al_2O_3$ | $Fe_2O_3$ | CaO | MgO | $Na_2O$ | $K_2O$ | MnO | $P_2O_5$ | $TiO_2$ | $V_2O_5$ | LOI | $CO_2$ | $SO_4^{2-}$ | $Cl^-$ | Reactivity |
|---|---|---|---|---|---|---|---|---|---|---|---|---|---|---|---|---|
| PZT | 49.98 | 16.25 | 4.02 | 2.41 | 1.33 | 4.62 | 4.79 | 0.174 | 0.09 | 0.62 | <0.003 | 14.96 | 1.36 | 0.10 | 0.11 | 70.25 |
| PZQ | 47.71 | 16.72 | 9.03 | 6.49 | 3.26 | 4.23 | 2.64 | 0.197 | 0.73 | 2.38 | 0.017 | 5.63 | 0.80 | 0.11 | 0.07 | 73.46 |
| F | 44,11 | 15.02 | 14.9 | 9.47 | 6.31 | 4.01 | 1.26 | 0.204 | 0.80 | 4.53 | <0.003 | 0.71 | – | <0.05 | 0.19 | 74.03 |
| PP | 37.58 | 12.63 | 7.83 | 19.37 | 2.78 | 3.33 | 1.38 | 0.150 | 0.78 | 2.03 | 0.017 | 11.27 | 4.62 | 0.91 | 0.05 | 58.04 |
| SF | 91.80 | 0.59 | 0.18 | 0.66 | 0.33 | 0.17 | 0.35 | 0.016 | 0.05 | 0.01 | <0.003 | 4.41 | 0.17 | 0.19 | 0.03 | 92.57 |

Note: $Co_3O_4 \leq 0.005$ %, CuO ≤ 0.005 %, NiO ≤ 0.003 %, $Cr_2O_3 \leq 0.01$ %; Reactivity: $SiO_2 + Al_2O_3 + Fe_2O_3$ (min of 70 % required).

analysis were compared with the chemical requirements in ASTM C 618 (ASTM, 2022). The combined amounts of $SiO_2 + Al_2O_3 +$ total $Fe_2O_3$, that play an important role in the occurrence of pozzolanic reactions, are greater than 70 %, except for the sample PP. All of the tuff samples investigated in this study also fulfill the chemical limitations for MgO, $SO_3$, and LOI, as shown in Table 8. All analyzed samples meet the ASTM specifications for minimum content of 70 %, except for the PP sample, which exceeds the maximum $SO_3$ content. It should be noted that the PZT and PP samples do not meet the LOI specifications for any of the three classes specified in the standard.

### 3.4. Pozzolanic activity and mechanical performance

Fig. 11 shows the results of determining the amount of calcium hydroxide contained in each of the tested samples after a fixed period of 7 days at a temperature of 40 °C. The test is considered positive when the concentration of calcium hydroxide in solution is lower than the saturation concentration. The results for the cement/additive mixture, expressed in mmol/L, pass the pozzolanicity test when the point on the graph is situated below the reference curve. From the tests on the activity of different additives, it is observed that, in ascending order of activity, the polishing powder, quarry pozzolan, and volcanic pozzolanic tuff exhibit pozzolanic activity. The resistance activity index (RAI) has been determined, which is one of the three specifications of UNE 80303–2:2017 (AENOR, 2017) that outlines how to use a pozzolanic material as an addition for common cements resistant to seawater. Following the test method of UNE-EN 196-1 (AENOR, 2018a) with a 75/25 cement/additive mass ratio, the compressive strength at 28 days should be equal to or greater than 75 % of the reference cement's strength, Type I/42.5R/SR. Fig. 12 demonstrates that all additives have surpassed the 75 % threshold of strength (green dashed line), with both pozzolan materials and silica fume notably exceeding the required 75 % strength.

In Fig. 13, the results obtained from measuring the flexural and compressive strengths in the mortars at 28 days are shown. All mortars manufactured with these additives meet the maximum compressive strength required for masonry mortars Md (>25 $N/mm^2$), allowing their use from mortars for partitions and partitions walls (M-5), exposed brickwork (M-7.5), reinforced and non-reinforced masonry structures

**Table 8**
$CO_2$-eq balance as a function of the parameters considered in the study.

| Concept | Gran Canaria ($kgCO_2$-eq/tonne of cement) | Tenerife ($kgCO_2$-eq/tonne of cement) |
|---|---|---|
| Cement emissions [EAS] | 125 | 125 |
| Emission reduction by eliminating 20 % of clinker [EAS] | −17 | −17 |
| Emission increase due to transport (50 km) (Shen et al., 2015; Government of Spain, 2010) | +1.58 | +1.58 |
| GHG increase due to crushing and mixing (9.3 kWh/tonne) (Porritt, 2009) and (Regional Government of the Canary Islands, 2025) | +1.01 | +1.06 |
| Total | 110.59 | 110.64 |

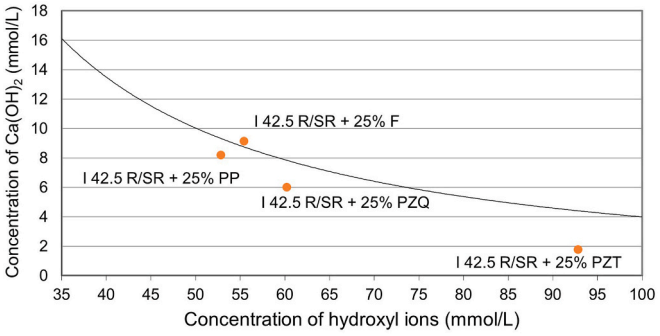


**Fig. 11.** Variation of the pozzolanic behaviour of the samples analyzed at 7 days compared to the reference cement I/42.5R/SR. Codes: (F) filler, (PP) polishing powder, (PZT) pozzolan tuff, and (PZQ) quarry pozzolan.

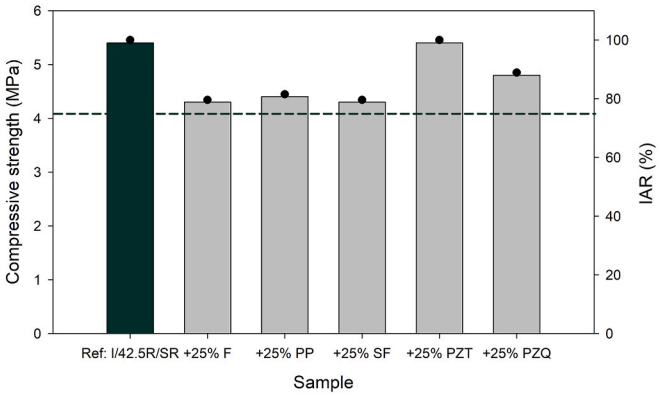


**Fig. 12.** Comparison of the resistance activity index (RAI) in mixtures of 75 % cement + 25 % additive with respect to the reference cement I/42.5R/SR. Codes: (F) filler, (PP) polishing powder, (SF) silica fume, (PZT) pozzolan tuff, and (PZQ) quarry pozzolan.

(M-7.5), high-strength masonry, and floors for ceramic and cementitious tiles, among others.

It should be noted that the resistance activity indices shown in Fig. 12 and the absolute flexural and compressive strengths presented in Fig. 13 represent different descriptors of mechanical performance, which are influenced not only by pozzolanic reactivity but also by dilution effects, particle size distribution, packing density, hydration kinetics, and cement strength class.

Mortars prepared with CEM II/A-P/42.5R cement (M1 series) exhibit higher strength values than those made with CEM IV/A-P/32.5N cement (M2 series). As expected, the partial replacement of cement by additives led to a reduction in compressive strength compared to the reference mortars (cf. Fig. 10). Among the evaluated additions, volcanic pozzolanic tuff showed the best mechanical performance, with decreases in strength ranging from 8 % to 22 %, followed by filler (11.73 % – 27.34 %) and silica fume (8.14 % – 39.56 %).

No significant differences were observed between using standardized aggregates and bagged aggregates from a local Canary quarry, with a

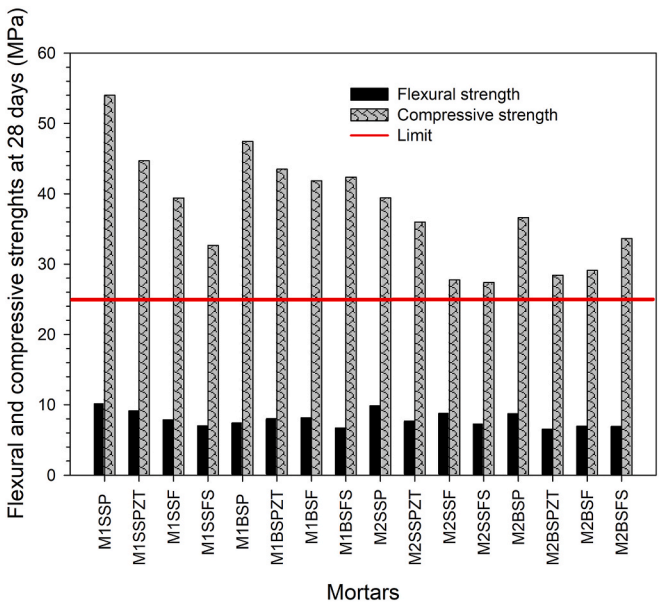


**Fig. 13.** Compressive and flexural strengths of the mortars at 28 days. The red line indicates the upper limit of 25 MPa for the compressive strength required for the mortars. Sample codes correspond to the classification of mortars given in Table 4. (For interpretation of the references to color in this figure legend, the reader is referred to the Web version of this article.)

decrease of 12 % in the case of M1SSP compared to M1SS and 7 % in the case of mortar M2BSP compared to M2SSP.

The reduction in compressive strength observed in the pozzolan-bearing mortars can be explained by the combined effect of several factors. First, the partial replacement of clinker introduces a dilution effect that reduces the amount of hydrated C–S–H formed at early ages. Second, the pozzolanic reactivity of the volcanic materials develops gradually, and therefore does not fully compensate the early-age dilution at 28 days. Third, differences in particle size distribution and specific surface area between the pozzolans and the Portland cement affect packing density and hydration kinetics. Finally, the mechanical response is conditioned by the cement strength class (CEM II/A-P/42.5R vs. CEM IV/A-P/32.5N), which establishes the baseline performance of the blended system. Despite these combined effects, all mortars exceeded the regulatory strength requirement for masonry mortars, confirming their technical suitability.

According to standard UNE-EN 998-2 (AENOR, 2018b), mortars are primarily classified based on their compressive strength. Although the incorporation of additive does not necessarily enhance mechanical strength, all mixtures exhibited compressive strength values exceeding the maximum requirement for any masonry used (Md > 25). Therefore, the proposed additives can be safely employed for the manufacture of mortars with both CEM II and CEM IV cements for all applications specified in UNE-EN 998-2 (AENOR, 2018b).

### 3.5. Life-cycle results and performance-normalized metrics

In 2022, the International Energy Agency Secretariat developed emission trends for cement based on the percentage of clinker. The threshold ranges from 125 to 40 kg of $CO_2$ equivalent ($CO_2$-eq) per tonne of cement (International Energy Agency, 2024). For a maximum reduction of 20 % of clinker by replacing it with pozzolanic materials from volcanic tuffs, a reduction of 125 kg of $CO_2$-eq per current tonne to 108 kg of $CO_2$-eq per tonne of modified cement could be obtained.

To assess the environmental impact and energy consumption of adding 20 % volcanic pozzolans to clinker, it is necessary to cover the entire transformation process, from the mining industry to the subsequent subprocesses (extraction, crushing, loading, and transport) that involve the volcanic pozzolans (de Brito and Kurda, 2021; Escamilla--Fraile et al., 2025). Other authors have conducted similar studies using alternative products added to cement, such as ash from coal-fired power plants or glass grinding waste. In both cases, the environmental impact of the material added to the cement is primarily related to transport, crushing, and mixing (Hossain et al., 2017).

The average fuel consumption for transporting raw materials and solid fuels by truck has been estimated at approximately 0.06 L of diesel per tonne of material per kilometer travelled (Shen et al., 2015). Specifically, for the distances between the quarry and the final mixer, an average distance of 50 km was considered for each of the two islands studied. The technical specifications for diesel and its emissions are 2640 g$CO_2$-eq/L (Government of Spain, 2010). $CO_2$-eq emissions are calculated per tonne of volcanic pozzolans transported 50 km. The $CO_2$-eq emissions from transporting 20 % of the volcanic pozzolans will be 1.58 kg$CO_2$-eq per tonne of cement.

The crushing of volcanic pozzolans requires approximately 9.3 kWh of energy consumption per tonne for processing and use as a complementary cementitious material in cement manufacturing (Porritt, 2009). Greenhouse gas (GHG) emissions per kWh generated depend on the energy mix of each island. GHG emissions (year 2023) per kWh are 543 g$CO_2$-eq/kWh in Gran Canaria and 572 g$CO_2$-eq/kWh in Tenerife (Regional Government of the Canary Islands, 2025). Table 8 shows a summary of the $CO_2$-eq balance obtained in this study.

In summary, the reduction would be 11.5 %. On a 1-tonne binder basis, the simplified cradle-to-gate assessment indicates approximately 11.5 % reduction in Global Warming Potential (GWP) when substituting 20 % of clinker with local volcanic pozzolans, considering typical quarry extraction/grinding and regional electricity generation mix. When converted to per $m^3$ mortar (using typical binder content) and normalized by compressive strength at 28 days, the SCM mixes remain competitive relative to baseline cement, evidencing an advantageous $CO_2$-to-performance ratio.

### 3.6. Implications for cleaner production

The incorporation of volcanic pozzolans as SCM presents a technically sound pathway to reducing the environmental footprint of cement production. The 20 % clinker substitution evaluated in this study yields a net reduction in GWP of approximately 11.5 % at the binder level, within a simplified cradle-to-gate framework, even when explicitly accounting for regional transport (50 km) and grinding energy demand (9.3 kWh/tonne). This reduction is primarily due to avoided process emissions associated with calcination and clinker formation, which globally account for approximately 65 % of $CO_2$ emissions in cement manufacturing (Barbhuiya et al., 2024). The strength-normalized $CO_2$ performance of the modified binders further confirms that the environmental gains do not compromise regulatory mechanical requirements.

From a cleaner production perspective, the valorization of quarry residues and natural volcanic materials aligns with the circular economy principles of resource efficiency, industrial symbiosis, and reduced dependence on primary raw materials (Domínguez-Herrera et al., 2023; Hernández-González and Barbero-Barrera, 2025). Under cut-off allocation, these geomaterials exhibit minimal upstream burdens and comparatively low embodied energy, resulting in a better environmental performance profile compared to virgin clinker. Furthermore, the identified environmental hotspots—transport and comminution—remain significantly below the energy intensity of clinker production, reinforcing the viability of the proposed approach within standard industrial operations.

The implications of these findings extend beyond the regional scale of the Canary Islands. Numerous volcanic regions worldwide (e.g., Italy, Iceland, Japan, Indonesia, the Pacific Ring of Fire, parts of Central and South America, and East Africa) possess abundant, underexploited pozzolanic deposits with comparable mineralogical reactivity.

Therefore, the methodological framework applied here —focused on partial clinker substitution, regionalized energy mixes, and performance-normalized $CO_2$ metrics— can be readily extrapolated to international contexts. In countries where clinker ratios remain above the European Union average (approximately 75–80 %), the relative decarbonization potential could be even greater. These insights support global policy recommendations aimed at accelerating the deployment of SCM as part of low-carbon cement strategies.

In addition to direct $CO_2$ reduction, volcanic pozzolans contribute to greater durability by refining pores and reducing permeability, potentially extending service life and reducing the life-cycle impacts associated with repair and replacement. This dual benefit —lower embodied emissions and improved durability— positions pozzolanic SCMs as a key enabler in the decarbonization pathways outlined by the IEA and the Global Cement and Concrete Association.

Overall, the integration of volcanic SCM represents a scalable and low-risk intervention, compatible with existing cement plant infrastructure. The results obtained in this study contribute to the international evidence base supporting clinker factor reduction and demonstrate that significant environmental gains can be achieved while maintaining performance and complying with standardized cement classifications. In this respect, the present study provides not only regional validation but also a transferable technological framework for implementing decarbonization strategies based on volcanic SCM in volcanic regions worldwide.

## 4. Conclusions

Unwelded ignimbrites of trachytic, phonolitic, or rhyolitic composition are salic pyroclastic rocks that exhibit excellent pozzolanic properties for the production of Portland cement. These materials are abundant in the Canary Islands, primarily found in the central islands of Tenerife and Gran Canaria, representing a strategically relevant indigenous supplementary cementitious material (SCM) resource.

All mortars manufactured using the standard dosages meet the maximum compressive strength requirement for masonry mortars Md (>25 $N/mm^2$). Mortars made with CEM II/A-P/42.5R exhibit higher strength values than those made with CEM IV/A-P/32.5N. Despite all additives causing a decrease in compressive strength, all values remain above the maximum required for masonry mortars, Md (>25 $N/mm^2$).

All additions surpassed the resistance activity index for seawater (RAI), fulfilling one of the three specifications outlined in UNE 80303–2:2017 (AENOR, 2017). Furthermore, almost all of the studied samples from the tuff from the volcanic zone have major chemical components, $SiO_2$ + $Al_2O_3$ + total $Fe_2O_3$ exceeding 70 %, conforming with the chemical requirements of ASTM and the Spanish regulations. The criteria for flexural and compressive strength were also satisfied, indicating that the region studied has a significant reserve potential for sustainable cement production.

Petrographic analysis of tuffs using optical microscopy, scanning electron microscopy (SEM–EDX), X-ray diffraction (XRD), and spectroscopic techniques proved to be effective, rapid and accessible tools for evaluating the suitability of pozzolanic cements. These techniques revealed the key petrographic, mineralogical, and textural characteristics that determine the technical performance of the resulting binders.

For a maximum 20 % reduction in clinker by replacing it with pozzolanic materials from volcanic tuffs, the simplified cradle-to-gate life cycle assessment (LCA) indicates that 11.5 % $CO_2$-eq could be saved per tonne of modified cement. The valorization of quarry residues directly contributes to the implementation of a circular economy and reduces the demand for virgin raw material extraction. These findings demonstrate a technically viable, low-carbon pathway for mortar production and provide direct support for cleaner production strategies in volcanic regions.

The novelty of this work lies in establishing a direct and experimentally validated relationship between the geological origin of volcanic pozzolans, their standardized mechanical performance as SCM, and their decarbonization potential quantified at the binder level. The proposed performance-normalized environmental approach allows for consistent integration of material performance and $CO_2$ mitigation. Beyond its regional relevance, this approach is fully transferable to other volcanic regions worldwide and provides a practical technological route for implementing clinker reduction strategies in insular and transport-sensitive territories, as part of global low-carbon cement production strategies.

## CRediT authorship contribution statement

**Juan J. Santana:** Writing – review & editing, Writing – original draft, Visualization, Validation, Supervision, Software, Resources, Project administration, Methodology, Investigation, Formal analysis, Data curation, Conceptualization. **Luis E. Hernández-Gutiérrez:** Writing – original draft, Supervision, Investigation, Formal analysis. **Ignacio Nuez:** Writing – original draft, Validation, Supervision, Methodology, Investigation, Formal analysis, Data curation. **Jiri Libich:** Validation, Software, Methodology, Data curation, Conceptualization. **Ricardo A. Liria-Romero:** Visualization, Validation, Software, Investigation, Formal analysis, Data curation. **Ricardo M. Souto:** Writing – review & editing, Writing – original draft, Visualization, Validation, Supervision, Software, Resources, Methodology, Investigation, Formal analysis, Data curation, Conceptualization.

## Declaration of competing interest

The authors declare that they have no known competing financial interests or personal relationships that could have appeared to influence the work reported in this paper.

## Acknowledgements

We gratefully acknowledge the assistance of the Advanced Confocal and Electronic Microscopy Service (SIMACE), University of Las Palmas de Gran Canaria (Canary Islands, Spain), for providing the high-resolution confocal images and the SEM-EDX analysis. We also wish to thank to Prof. Óscar González from the CIDIA Research Group from the University of Las Palmas de Gran Canaria (Canary Islands, Spain) for the XRD analysis and for assistance in the interpretation of the results.

## Data availability

Data will be made available on request.

## References

Ababneh, A., Matalkah, F., 2018. Potential use of Jordanian volcanic tuffs as supplementary cementitious materials. Case Stud. Constr. Mater. 8, 193–202. https://doi.org/10.1016/j.cscm.2018.02.004.

Abiodun, Y.O., Olanrewaju, O.A., Gbenebor, O.P., Ochulor, E.F., Obasa, D.V., Adeosun, S.O., 2022. Cutting cement industry $CO_2$ emissions through Metakaolin use in construction. Atmosphere (Basel) 13, 1494. https://doi.org/10.3390/atmos13091494.

AENOR, 2025. UNE-EN 1097-6:2025. Tests for Mechanical and Physical Properties of Aggregates - Part 6: Determination of Particle Density and Water Absorption. AENOR, Madrid, Spain.

AENOR, 2020. UNE-EN 1015-11:2020. Methods of Test for Mortar for Masonary - Part 11: Determination of Flexural and Compressive Strength of Hardened Mortar. AENOR, Madrid, Spain.

AENOR, 2018a. UNE-EN 196-1:2018. Methods of Testing Cement - Part 1: Determination of Strength. AENOR, Madrid, Spain.

AENOR, 2018b. UNE-EN 998-2:2018. Specification for Mortar for Masonry - Part 2: Masonry Mortar. AENOR, Madrid, Spain.

AENOR, 2017a. UNE 80303-2:2017. Cements with Additional Characteristics. Part 2: Sea Water Resisting Cements. AENOR, Madrid, Spain.

AENOR, 2017b. UNE-EN 196-3:2017. Methods of Testing Cement. Part 3: Determination of Setting Times and Soundness. AENOR, Madrid, Spain.

AENOR, 2012a. UNE-EN 933-1:2012. Tests for Geometrical Properties of Aggregates - Part 1: Determination of Particle Size Distribution - Sieving Method. AENOR, Madrid, Spain.
AENOR, 2012b. UNE-EN 933-3:2012. Tests for Geometrical Properties of Aggregates - Part 3: Determination of Particle Shape - Flakiness Index. AENOR, Madrid, Spain.
AENOR, 2011a. UNE-EN 197-1:2011. Cement - Part 1: Composition, Specifications and Conformity Criteria for Common Cements. AENOR, Madrid, Spain.
AENOR, 2011b. UNE-EN 196-5. Methods of Testing Cement - Part 5: Pozzolanicity Test for Pozzolanic Cement. AENOR, Madrid, Spain.
AENOR, 2010. UNE-EN 1744-1:2010+A1:2013. Tests for Chemical Properties of Aggregates - Part 1: Chemical Analysis. AENOR, Madrid, Spain.
AENOR, 2000. UNE-EN 933-8:2000. Tests for geometrical properties of aggregates. Part 8: assessment of fines. Sand Equivalent Test. AENOR, Madrid, Spain.
Ahmadi, B., Shekarchi, M., 2010. Use of natural zeolite as a supplementary cementitious material. Cem. Concr. Compos. 32, 134–141. https://doi.org/10.1016/j.cemconcomp.2009.10.006.
Alonso Blanco, J.J., 1989. Estudio Volcanoestratigráfico y Volcanológico de los Piroclastos Sálicos del Sur de Tenerife. Secretariado de Publicaciones. Universidad de La Laguna, La Laguna, Spain.
Amran, M., Makul, N., Fediuk, R., Lee, Y.H., Vatin, N.I., Lee, Y.Y., Mohammed, K., 2022. Global carbon recoverability experiences from the cement industry. Case Stud. Constr. Mater. 17, e01439. https://doi.org/10.1016/j.cscm.2022.e01439.
Ancochea, E., Fuster, J., Ibarrola, E., Cendrero, A., Coello, J., Hernan, F., Cantagrel, J.M., Jamond, C., 1990. Volcanic evolution of the island of Tenerife (Canary Islands) in the light of new K-Ar data. J. Volcanol. Geoth. Res. 44, 231–249. https://doi.org/10.1016/0377-0273(90)90019-C.
ASTM, 2022. ASTM C618-22(2022), Standard Specification for Coal Fly Ash and Raw or Calcined Natural Pozzolan for Use in Concrete. West Conshohocken, PA, USA.
ASTM, 2013. ASTM C311/C311M−13. Standard Test Methods for Sampling and Testing Fly Ash or Natural Pozzolans for Use in Portland-Cement Concrete. West Conshohocken, PA, USA.
Barbhuiya, S., Kanavaris, F., Das, B.B., Idrees, M., 2024. Decarbonising cement and concrete production: strategies, challenges and pathways for sustainable development. J. Build. Eng. 86, 108861. https://doi.org/10.1016/j.jobe.2024.108861.
Barcelo, L., Kline, J., Walenta, G., Gartner, E., 2014. Cement and carbon emissions. Mater. Struct. 47, 1055–1065. https://doi.org/10.1617/s11527-013-0114-5.
Barrera Morate, J.L., García Moral, R., 2011. Mapa Geológico de Canarias, first. ed. GRAFCAN, Santa Cruz de Tenerife, Spain.
Çavdar, A., Yetgin, Ş., 2007. Availability of tuffs from northeast of Turkey as natural pozzolan on cement, some chemical and mechanical relationships. Constr. Build. Mater. 21, 2066–2071. https://doi.org/10.1016/j.conbuildmat.2006.05.034.
Coello, J., Cantagrel, J.-M., Hernán, F., Fúster, J.-M., Ibarrola, E., Ancochea, E., Casquet, C., Jamond, C., Díaz de Téran, J.-R., Cendrero, A., 1992. Evolution of the eastern volcanic ridge of the Canary Islands based on new K-Ar data. J. Volcanol. Geoth. Res. 53, 251–274. https://doi.org/10.1016/0377-0273(92)90085-R.
Costafreda, J.L., Martín, D.A., Presa, L., Parra, J.L., 2021. Altered volcanic tuffs from los frailes caldera. A study of their pozzolanic properties. Molecules 26, 1–17. https://doi.org/10.3390/molecules26175348.
de Brito, J., Kurda, R., 2021. The past and future of sustainable concrete: a critical review and new strategies on cement-based materials. J. Clean. Prod. 281, 123558. https://doi.org/10.1016/j.jclepro.2020.123558.
Dedeloudis, C., Zervaki, M., Sideris, K., Juenger, M., Alderete, N., Kamali-Bernard, S., Villagrán, Y., Snellings, R., 2018. Natural pozzolans. In: De Belie, N., Soutsos, M., Gruyaert, E. (Eds.), Properties of Fresh and Hardened Concrete Containing Supplementary Cementitious Materials. RILEM state-of-the-art Reports, vol. 25. Springer, Cham, Switzerland, pp. 181–231. https://doi.org/10.1007/978-3-319-70606-1_6.
Domínguez-Herrera, M.M., González-Morales, O., González-Díaz, E., 2023. Social responsibility of construction company as strategy for sustainability in island territories. Constr. Econ. Build. 23, 31–55. https://doi.org/10.5130/AJCEB.v23i1/2.8163.
Escamilla-Fraile, S., Cruz-González, R.L., García-Afonso, O., Calero-García, F.J., González-Díaz, B., Ramos-Real, F.J., 2025. Scenario-based analysis of energy transition for an outermost EU territory: the case of Tenerife island. Energy Convers. Manag. X. 26, 100917. https://doi.org/10.1016/j.ecmx.2025.100917.
Fan, C., Miller, S.A., 2018. Reducing greenhouse gas emissions for prescribed concrete compressive strength. Constr. Build. Mater. 167, 918–928. https://doi.org/10.1016/j.conbuildmat.2018.02.092.
Fazilati, M., Mohammadi Golafshani, E., 2020. Durability properties of concrete containing amorphous silicate tuff as a type of natural cementitious material. Constr. Build. Mater. 230, 117087. https://doi.org/10.1016/j.conbuildmat.2019.117087.
González-Morales, O., Peña-Vázquez, R., González-Díaz, E., Rodríguez-Donate, M.C., Alonso Gutiérrez, L.C., 2025. Public policies for the design and implementation of sustainable cities. Sustainability 17, 9782. https://doi.org/10.3390/su17219782.
Government of Spain, 2010. Royal Decree 1088/2010 Modifying Royal Decree 61/2006, of 31 January with Regards the Technical Specifications of Gasolines, Gas Oils, Use of Biofuels and Sulphur Content of Fuels for Marine Use, BOE-A-2010. Boletín Oficial del Estado, Madrid, Spain.
Hernán, F., 1976. Estudio petrológico y estructural del complejo traquítico-sienítico de Gran Canaria. Esfurlios Geol. 36, 95–73.
Hernández, L.E., Eff-Darwich, A., Viñas, R., Rodríguez-Losada, J.A., 2011. Radiology of Canarian volcanic rocks. In: Qian, Q., Zhou, Y. (Eds.), Harmonising Rock Engineering and the Environment - Proceedings of the 12th ISRM International Congress on Rock Mechanics. CRC Press, Beijing, China, pp. 641–644.
Hernández González, R., Barbero-Barrera, M.M., 2025. Paradigm shift in the construction sector: evolution of the sector towards industrialisation and circular economy. Anales de Edificación 11 (1), 42–49. https://doi.org/10.20868/ade.2025.5518.
Hernández González, R., Barbero Barrera, M.M., 2023. Island regions and self-sufficient to reduce the environmental footprint. Anales de Edificación 9 (3), 38–45. https://doi.org/10.20868/ade.2023.5378.
Hernández Gutiérrez, L.E., 2014. Geomechanical characterization of volcanic rocks of the Canary Islands. Universidad de La Laguna, La Laguna, Spain. https://doi.org/10.13140/2.1.2526.2884.
Hossain, M.U., Poon, C.S., Lo, I.M.C., Cheng, J.C.P., 2017. Comparative LCA on using waste materials in the cement industry: a Hong Kong case study. Resour. Conserv. Recycl. 120, 199–208. https://doi.org/10.1016/j.resconrec.2016.12.012.
Hunyak, O., Sobol, K., Markiv, T., Bidos, V., 2019. The effect of natural pozzolans on properties of vibropressed interlocking concrete blocks in different curing conditions. Prod. Eng. Arch. 22, 3–6. https://doi.org/10.30657/pea.2019.22.01.
International Energy Agency, 2024. Definitions for near-zero and low emissions steel and cement, and underlying emissions measurement methodologies. Summary of Emerging Understandings. IEA, Paris, France. https://www.iea.org/reports/definitions-for-near-zero-and-low-emissions-steel-and-cement-and-underlying-emissions-measurement-methodologies.
Janotka, I., Krajči, L., 2003. Utilization of Natural Zeolite in Portland Cement of Increased Sulphate Resistance, 221. ACI Spec. Publ., pp. 223–229
Kushnir, A.R.L., Heap, M.J., Griffiths, L., Wadsworth, F.B., Langella, A., Baud, P., Reuschlé, T., Kendrick, J.E., Utley, J.E.P., 2021. The fire resistance of high-strength concrete containing natural zeolites. Cem. Concr. Compos. 116, 103897. https://doi.org/10.1016/j.cemconcomp.2020.103897.
Le Maitre, R.W., Streckeisen, A., Zanettin, B., Le Bas, M.J., Bonin, B., Bateman, P. (Eds.), 2002. Igneous Rocks: a Classification and Glossary of Terms, second ed. Cambridge University Press, Cambridge, UK. https://doi.org/10.1017/CBO9780511535581.
Markiv, T., Sobol, K., Franus, M., Franus, W., 2016. Mechanical and durability properties of concretes incorporating natural zeolite. Arch. Civ. Mech. Eng. 16, 554–562. https://doi.org/10.1016/j.acme.2016.03.013.
Mertens, G., Snellings, R., Van Balen, K., Bicer-Simsir, B., Verlooy, P., Elsen, J., 2009. Pozzolanic reactions of common natural zeolites with lime and parameters affecting their reactivity. Cement Concr. Res. 39, 233–240. https://doi.org/10.1016/j.cemconres.2008.11.008.
Miller, S.A., Horvath, A., Monteiro, P.J.M., 2016. Readily implementable techniques can cut annual $CO_2$ emissions from the production of concrete by over 20%. Environ. Res. Lett. 11, 074029. https://doi.org/10.1088/1748-9326/11/7/074029.
Moumin, G., Ryssel, M., Zhao, L., Markewitz, P., Sattler, C., Robinius, M., Stolten, D., 2020. $CO_2$ emission reduction in the cement industry by using a solar calciner. Renew. Energy 145, 1578–1596. https://doi.org/10.1016/j.renene.2019.07.045.
Najimi, M., Jamshidi, M., Pourkhorshidi, A., 2008. Durability of concretes containing natural pozzolan. Proc. Inst. Civ. Eng. Constr. Mater. 161, 113–118. https://doi.org/10.1680/coma.2008.161.3.113.
Nature, 2021. Concrete needs to lose its colossal carbon footprint, 2021. Nature 597, 593–594. https://doi.org/10.1038/d41586-021-02612-5.
Neupane, K., 2022. Evaluation of environmental sustainability of one-part geopolymer binder concrete. Clean. Mater. 6, 100138. https://doi.org/10.1016/j.clema.2022.100138.
Papadakis, V.G., Tsimas, S., 2002. Supplementary cementing materials in concrete: part I. Efficiency and design. Cement Concr. Res. 32, 1525–1532. https://doi.org/10.1016/S0008-8846(02)00827-X.
Porritt, J., 2009. The Concrete Industry Sustainability Performance Report (2009). The Concrete Centre, Camberley, UK. https://www.concretecentre.com/TCC/media/TCCMediaLibrary/Products/MB_First_Concrete_Performance_Report_Mar09.pdf.
Presa, L., Rosado, S., Peña, C., Martín, D.A., Costafreda, J.L., Astudillo, B., Parra, J.L., 2023. Volcanic ash from the Island of La Palma, Spain: an experimental study to establish their properties as pozzolans. Processes 11, 657. https://doi.org/10.3390/pr11030657.
Qaidi, S., Najm, H.M., Abed, S.M., Ahmed, H.U., Al Dughaishi, H., Al Lawati, J., Sabri, M. M., Alkhatib, F., Milad, A., 2022. Fly ash-based geopolymer composites: a review of the compressive strength and microstructure analysis. Materials (Basel) 15, 1–41. https://doi.org/10.3390/ma15207098.
Rakhimov, R.Z., Rakhimova, N.R., Gaifullin, A.R., Morozov, V.P., 2017. Properties of Portland cement pastes enriched with addition of calcined marl. J. Build. Eng. 11, 30–36. https://doi.org/10.1016/j.jobe.2017.03.007.
Regional Government of the Canary Islands, 2025. Canary annual energy plan. Gobierno De Canarias. Las Palmas de Gran Canaria, Spain.
Report International Energy Agency (IEA), 2023. Cement, Net Zero Emissions Guide 2023. IEA, Paris, France. https://www.iea.org/reports/cement-3.
Rodríguez-Losada, J.A., Hernández-Gutiérrez, L.E., Olalla, C., Perucho, A., Serrano, A., Eff-Darwich, A., 2009. Geomechanical parameters of intact rocks and rock masses from the Canary Islands: implications on their flank stability. J. Volcanol. Geoth. Res. 182, 67–75. https://doi.org/10.1016/j.jvolgeores.2009.01.032.
Rojas, M.F., Cabrera, J., 2002. The effect of temperature on the hydration rate and stability of the hydration phases of metakaolin–lime–water systems. Cement Concr. Res. 32, 133–138. https://doi.org/10.1016/S0008-8846(01)00642-1.
Sammer, T., Nasiri, A., Kostoglou, N., Ravi, K., Raith, J.G., 2024. Insight into carbon black and silica fume as cement additives for geoenergy wells: linking mineralogy to mechanical and physical properties. C (Basel) 10, 71. https://doi.org/10.3390/c10030071.
Santana, J.J., Rodríguez-Brito, N., Blanco-Peñalver, C., Mena, V.F., Souto, R.M., 2022. Durability of reinforced concrete with additions of natural pozzolans of volcanic origin. Materials (Basel) 15, 8352. https://doi.org/10.3390/ma15238352.

Schmincke, H.-U., Sumita, M., 2010. Geological Evolution of the Canary Islands: a Young Volcanic Archipelago Adjacent to the Old African Continent. Görres Druckerei und Verlag, Koblenz, Germany.

Schmincke, H.U., 1967. Cone sheet swarm, resurgence of tejeda caldera, and the early geologic history of gran Canaria. Bull. Volcanol. 31, 153–162. https://doi.org/10.1007/BF02597011.

Shen, W., Cao, L., Li, Q., Zhang, W., Wang, G., Li, C., 2015. Quantifying $CO_2$ emissions from China's cement industry. Renew. Sustain. Energy Rev. 50, 1004–1012. https://doi.org/10.1016/j.rser.2015.05.031.

Shi, C., 1998. Pozzolanic reaction and microstructure of chemical activated lime-fly ash pastes. ACI Mater. J. 95, 537–545. https://doi.org/10.14359/396.

Sobol, K., Markiv, T., Terlyha, V., Franus, W., 2015. Peculiarities of hydration processes of cements containing natural zeolite. Bud. i Archit. 14, 105–113. https://doi.org/10.35784/bud-arch.1674.

Summerbell, D.L., Barlow, C.Y., Cullen, J.M., 2016. Potential reduction of carbon emissions by performance improvement: a cement industry case study. J. Clean. Prod. 135, 1327–1339. https://doi.org/10.1016/j.jclepro.2016.06.155.

Tayeh, B.A., Hamada, H.M., Almeshal, I., Bakar, B.H.A., 2022. Durability and mechanical properties of cement concrete comprising pozzolanic materials with alkali-activated binder: a comprehensive review. Case Stud. Constr. Mater. 17, e01429. https://doi.org/10.1016/j.cscm.2022.e01429.

Türkmenoğlu, A.G., Tankut, A., 2002. Use of tuffs from central Turkey as admixture in pozzolanic cements: assessment of their petrographical properties. Cement Concr. Res. 32, 629–637. https://doi.org/10.1016/S0008-8846(01)00734-7.

Wasim, M., Abadel, A., Abu Bakar, B.H., Alshaikh, I.M.H., 2022. Future directions for the application of zero carbon concrete in civil engineering – a review. Case Stud. Constr. Mater. 17, e01318. https://doi.org/10.1016/j.cscm.2022.e01318.

Xia, J., Guan, Q., Zhou, Y., Wang, J., Gao, C., He, Y., Wang, Z., Song, P., 2021. Use of natural pozzolans in high-performance concrete for the Mombasa–Nairobi railway. Adv. Cement Res. 33, 318–330. https://doi.org/10.1680/jadcr.20.00045.

Zhang, L., Mabee, W.E., 2016. Comparative study on the life-cycle greenhouse gas emissions of the utilization of potential low carbon fuels for the cement industry. J. Clean. Prod. 122, 102–112. https://doi.org/10.1016/j.jclepro.2016.02.019.

Zhang, M.H., Malhotra, V.M., 1995. Characteristics of a thermally activated alumino-silicate pozzolanic material and its use in concrete. Cement Concr. Res. 25, 1713–1725. https://doi.org/10.1016/0008-8846(95)00167-0.